First-principles study on the effect of doping ratio of La/Ir co-doping on electronic and magneto-optic properties of $SrTiO_3$

YUEQIN WANG*, WEIBO HU, JINYANG WANG, LILI ZHENG, FUZHANG CHEN
School of Mechanics and Optoelectronic Physics, Anhui University of Science and Technology, Huainan 232001, China

The effects of different doping ratio of La/Ir co-doping on magnetic and optical properties of $SrTiO_3$ (STO) are investigated by first-principles calculations. The average magnetic moments of 2:1-La/Ir-STO and 1:2-La/Ir-STO are 0.67 μ_B/supercell and 1.0 μ_B/supercell, which increases with the increasing of doping concentration of Ir atoms. The net magnetic moment of 1:1-La/Ir-STO is zero due to the charge compensation of the system. Both the 1:1-La/Ir-STO and 2:1-La/Ir-STO co-doped systems have two obvious absorption peaks, showing good visible light absorption performance, and the 1:1-La/Ir-STO exhibits higher photocatalytic activity than that of 2:1-La/Ir-STO co-doped system.

(Received June 19, 2023; accepted February 9, 2024)

Keywords: Doping ratio, Photocatalytic activity, Magnetic moment, First-principles calculations

1. Introduction

La-$SrTiO_3$ based oxide is a typical *n*-type donor doped semiconductor, which has been widely used in IT-SOFCs anode materials, thermoelectric ceramics and catalysis due to its high dielectric, great conductivity and optical performance [1]. However, there are surplus hole defect in La-$SrTiO_3$ system, limiting its application in catalytic region.

How to effectively suppress the hole defect in La-$SrTiO_3$ based materials has attracted extensive interest of researchers. It has been revealed that the concentration of defects can be effectively suppressed by advanced preparation technology. Keeble et al. [2] have prepared La-$SrTiO_3$ thin films by molecular beam epitaxy. It is found that the concentration of Sr vacancy and cluster defects in the film was shown to be one order-of-magnitude lower than that of theoretical data. In addition, the doping concentration of La element can also changes internal defects and shows a significant effect on the photocatalytic activity [3]. Li et al. [4] reported that the photocatalytic activity of La-$SrTiO_3$ increases first and then decreases with the increasing of La doping concentration. The catalytic efficiency can be reached the highest as the doping concentration up to 0.5%. There have been found that La co-doped with other metal elements can inhibit the formation of vacancy defects [5,6]. The La co-doped with the metals of Cr, Co, Rh, Mn and Ni are revealed to play significant synergistic effect on the electronic structure and optical properties [7]. Recently, Modak [8] investigated the effect of co-doping with B, Al, La and Cr into Ir-doped $SrTiO_3$, revealing all these four codopant play different role in enhancing its photocatalytic activity. However, no relevant of the doping ratio of La and Ir co-doping on the magnetic and catalytic properties of $SrTiO_3$ has been reported.

In present work, we performed first principles studies on the electronic, magnetic-optical properties of La/Ir co-doped $SrTiO_3$ with consideration of different doping concentration. It was found that the introduction of Ir can enhance the magnetic moment and further expand the light absorption. The average magnetic moment increases with increasing Ir doping ratio. Our prediction calculations demonstrate that the dilute magnetic behavior in perovskite $SrTiO_3$ would be improved by combining La/Ir synergistic co-doping and different doping concentration.

2. Computation method

We selected the projector augmented wave (PAW) method to perform our first-principles calculations with the general gradient approximation plus the on-site repulsion (GGA+U), implemented in the CASTEP codes. We used the on-site repulsion U_{eff} = 2.3 eV, 8 eV, 7.5 eV and 2 eV on the Ti-3*d*, O-2*p*, La-4*f* and Ir-5*d* states as previous theoretical studies [9,10]. We used the energy cutoff of 400 eV for the plane wave expansion of the PAW. All calculated structures were relaxed in a 5×5×5 *k*-points until all the component residual forces are smaller than 1×10^{-3} eV/Å.

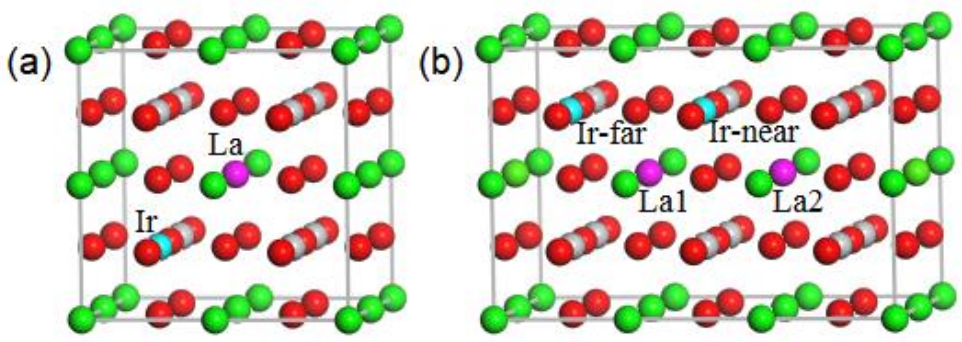

Fig. 1. Crystal structures of 1:1-La/Ir-STO and 2:1-La/Ir-STO. The green, gray and red ball represent as Sr, Ti and O atoms (color online)

To simulate the effect of different doping concentration on the electronic structure of La/Ir codoped $SrTiO_3$ systems, here we built the 2×2×3, 2×2×2 and 2×2×1 supercell based on the optimized primitive cell, respectively. The corresponding doping concentration are denote as 8.33%, 12.5% and 25%, respectively. The two main doping structures of 1:1-La/Ir-STO and 2:1-La/Ir-STO are plotted in Fig. 1.

The optical coefficient $\alpha(\omega)$ is described by the following equation [11,12]

$$\alpha(\omega)=\sqrt{2}\omega\left[\sqrt{\varepsilon_1(\omega)^2+\varepsilon_2(\omega)^2}-\varepsilon_1(\omega)\right]^{1/2}=2\omega k(\omega) \tag{1}$$

where ε_1 and ε_2 are the real and imaginary parts of dielection function, ω is phonon angular frequency and $k(\omega)$ is extinction coefficient.

3. Results and discussion

The electronic structure of La/Ir mono-doped 2×2×2 supercell were calculated and shown in Fig. 2. The Fermi level of La-STO is located at the conduction band, due to the dopant La has one more electron than that of the host Sr site, showing *n*-type semiconductor characteristic. The band gap between valence band top and the occupied impurity state of La-STO is 3.533 eV, which is higher than that of perfect STO. La doping will lead to a blue shift of light absorption, which is consistent with the experiment results [13]. The density of states (DOS) of La mainly appear in the low energy valence band and the high energy conduction band due to the La-O ionic bond. The Fermi level of Ir-STO locates at the center between the valence band and conduction band, showing a *p*-type semiconductor nature.

There are continuous impurity states at the top of valence band and the bottom of conduction band. These impurity states are composed of Ir 5*d* and O 2*p* states, indicating a strong Ir-O covalent bond in Ir-STO configuration. Both the valence band and the conduction band shift towards the low energy direction, and the band gap reduces to 1.649 eV. It shows that the Ir-5*d* states mainly distribute in the partially occupied and non-occupied regions, which can be explained by the fact that the Ir dopant is more likely to display +4 oxidation state (including unpaired electrons $5d^5$).

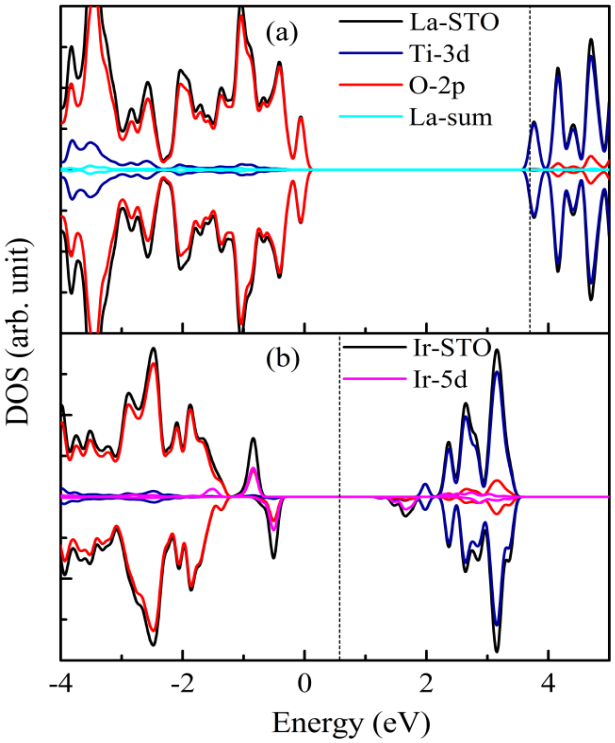

Fig. 2. Density of states of La-STO (a) and Ir-STO (b) (color online)

The density of states of perfect STO and La/Ir-STO are shown in Fig. 3. The valence band and conduction band of STO are composed of O 2*p* states and Ti 3*d* states, respectively. In the case of La/Ir co-doping, the valence band and conduction band move towards the low energy direction, resulting in a significantly narrow band gap. The

decreased band gap is ascribe to the transition of Ir 5*d* and O 2*p* hybrid states to the forbidden band, thus lead to a small band gap of about 1.872 eV. The narrowed band gap is beneficial to suppress the recombination of photo-generated electron-hole pair, thus photon excitation energy is reduced. The hybridization of Ir-O is become strong in the La/Ir co-doped system, especially in the valence band, while the hybridization of Ti 3*d* and O 2*p* are weakened.

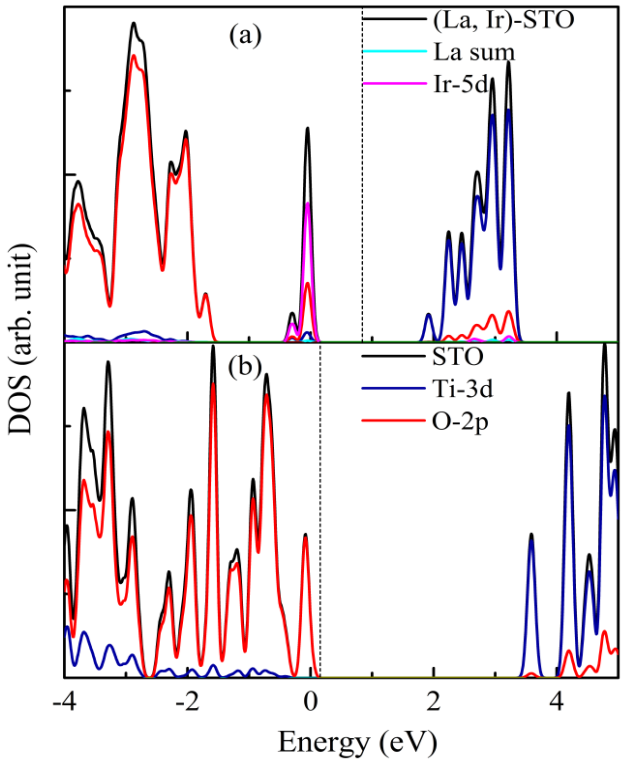

Fig. 3. Density of states of 1:1-La/Ir-STO (a) and STO (b) (color online)

To determine the effect of doping concentration on electronic structure, the DOS of three doping systems with concentration of 8.33%, 12.5% and 25% are shown in Fig. 4. The valence band and conduction band of all three configurations shift towards low energy, and the more obvious it moves with the increase of doping concentration. The DOS of 8.33%-La/Ir-STO and 12.5%-La/Ir-STO co-doped systems are almost the same. Some isolate impurity electronic states appear at the Fermi level. These partially unoccupied and occupied states originate from the Ir 5*d* and O 2p states. The contribution of La to the DOS can almost negligible. The DOS of 8.33%-La/Ir-STO co-doped system is relatively localized, and the Ti 3*d* and O 2*p* states become more delocalized with the increase of doping concentration, which may be caused by the weakening of Ti-O hybridization. In addition, it is noted that the band gaps decrease with the increasing of doping concentration, which are ascribed to the different location (Ti 3*d* states) of the conduction band minimum.

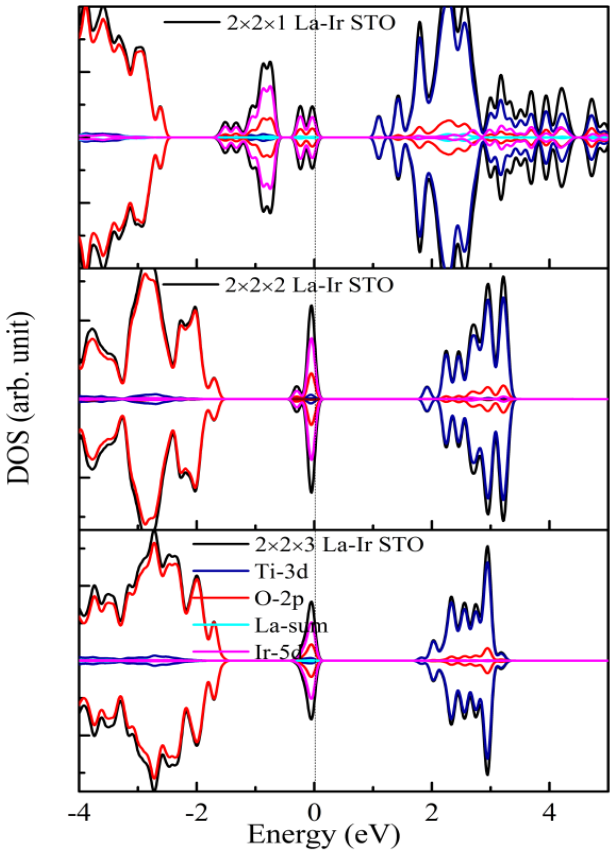

Fig. 4. Density of states of La/Ir-STO systems within different doping content (color online)

When the doping concentration increases to 25%, there are new impurity states generate in the mid-gap of La/Ir-STO, and the conduction band is more close to the Fermi level as compared with 8.33%-La/Ir-STO and 12.5%-La/Ir-STO, thus the band gap decreases significantly. The band gap of co-doped system with doping concentration 8.33% and 12.5% are both 1.8 eV, indicating that low doping concentration has little effect on band structure. Therefore, in the following section, the electronic structures of the 8.33%-La/Ir-STO system with different doping ratios are systematically calculated and discussed.

The total and partial DOS of La/Ir-STO with different Ir doping concentration are considered, as shown in Fig. 5. Firstly, the co-doped system with La:Ir concentration ratio of 2:1 is discussed. Within a 2×2×3 supercell model, two La and one Ir atoms are replaced at two Sr and one Ti sites, respectively (La:16.67%, Ir:8.33%). This type of replacement has two different configurations due to the relatively substitution sites. The calculated distance of La-La are 3.935 Å in the nearest neighbor (“near” structure) configuration and 5.583 Å in the second nearest neighbor (“far” structure) configuration. The distances of La-Ir in both configurations are 3.411 Å and 3.466 Å, respectively. The energy difference between the “near” and the “far” structures is 0.019 eV, while the

energy of the nearest neighbor configuration is relatively high. The conduction band of the near configuration is completely asymmetric, resulting in a magnetic moment of 0.65 μ_B/supercell. The valence band and conduction band of the second nearest neighbor configuration are completely symmetrical, generating a magnetic moment of about 0.69 μ_B/supercell, which is mainly due to the magnetization of Ti atoms. We can deduce that two La and one Ir are more likely to occupy the position of the next nearest neighbor.

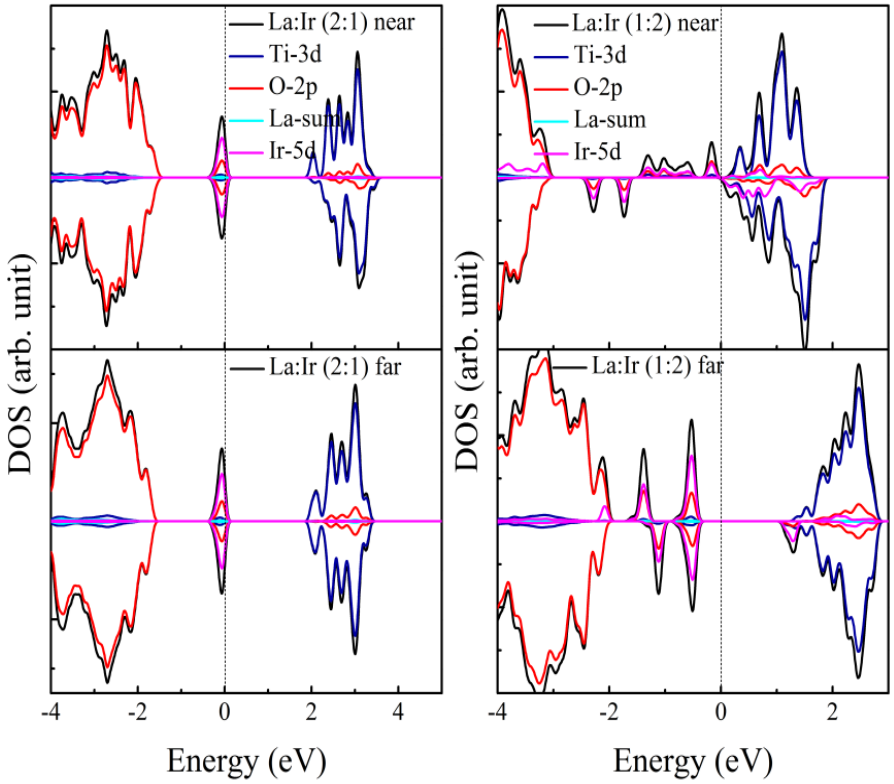

Fig. 5. Density of states of La/Ir-STO systems within different doping ratios (color online)

In addition, the electronic structures of one La and two Ir substituted at Sr and Ti sites are also discussed. The doping ratio of La and Ir is 1:2 (La:8.33%, Ir:16.67%), which also has two substitution structures. The optimized distance of Ir-Ir are 4.0 Å in the nearest neighbor structure and 5.638 Å in the second nearest neighbor structure, respectively. The distance of La-Ir are 3.433 Å and 3.436 Å in the above doped structures, respectively. The energy of the nearest neighbor structure is 0.103 eV higher than that of the second nearest neighbor structure. When the La:Ir doping ratio is 1:2, the nearest neighbor structure displays *n*-type doping with half-metallic nature. The majority spin DOS passes through the Fermi level, showing metallic properties, while the minority spin DOS is characterized by insulating band gap. That is to say, the phase transition in the nearest neighbor structure will lead to the photocatalytic deactivation. The partial DOS in the conduction band is completely asymmetric, resulting in a total magnetic moment of 1.01 μ_B/supercell, which is mainly contributed by the magnetization of Ti and O atoms. The Fermi level of the second nearest neighbor structure with 1:2 doping ratio is located in the forbidden band, and the top of valence band forms a continuous impurity state, resulting in the reduction of the band gap. The DOS of Ti 3*d* and O 2*p* have little contribution to the magnetic moment because the valence and conduction bands are completely symmetrical. The total moment is 0.99 μ_B/supercell, which is mainly originated from the spin of metal Ir dopant.

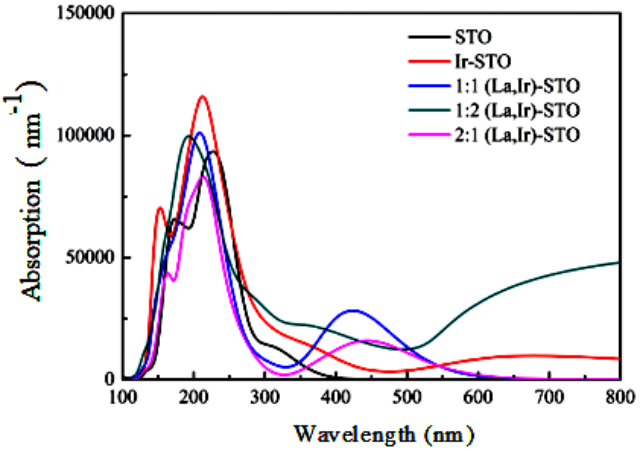

Fig. 6. Optical absorption of La/Ir co-doped STO within different doping ratios (color online)

Based on the above calculated electronic structure, the optical absorption properties of Ir-STO and La/Ir co-doped STO systems with different doping ratios are studied and shown in Fig. 6. The absorption of Ir-STO increases obviously due to the reduction of band gap after doping. The doping system shows new absorption peak in the visible light region and induces obvious red shift of the absorption edge, which is benefit for the enhancement of catalytic activity.

Both the 1:1-La/Ir-STO and 2:1-La/Ir-STO co-doped systems have two obvious absorption peaks, and the maximum absorption edge can be extended to 620 nm. The 2:1-La/Ir-STO co-doped system is charge imbalance, thus the Ir atoms coexist with +3 and +4 oxidation state to balance excess electron introduced by two La substitutions. In the case of 1:1-La/Ir-STO co-doped system, the Ir dopant is more likely to substitute at Ti site with +3 valence due to the charge compensation. The 1:1-La/Ir-STO has higher photocatalytic activity than that of 2:1-La/Ir-STO co-doped system. Therefore, the defect impurity states in 1:1-La/Ir-STO are passivated, which can effectively inhibit the recombination of electron-hole pairs and improve the catalytic activity.

4. Conclusions

The effects of different doing concentration and doping ratio on the electronic structure magnetic and optical properties are calculated by GGA+U_p+U_d method. Band gap of La/Ir-STO is almost the same as the doping concentration is lower than 12.5%. The total net magnetic moment of 1:1-La/Ir-STO is zero due to the charge compensation in system. The magnetization of Ti and O in 2:1-La/Ir-STO system produces magnetic moment of 0.65~0.69 μ_B/supercell. The average magnetic moment of 1:2-La/Ir-STO is 1.0 μ_B/supercell, which is derived from the contribution of Ir atom. The absorption edge of La/Ir-STO has obvious red shift, showing good visible light absorption performance.

Acknowledgement

This work was supported by the Key Projects of Support Program for Outstanding Young Talents in Colleges and Universities of Anhui Province (Grant No. gxyq2022018), the Key Research and Development and Achievement Transformation Project of Wuhu City (Grant No. 2023yf030) and the Talent Introduction Project of Anhui University of Science and Technology.

References

[1] X. Zhou, N. Yan, K. Chuang, RSC Adv. **4**, 118 (2013).
[2] D. J. Keeble, B. Jalan, L. Ravelli, W. Egger, G. Kanda, S. Stenner, Appl. Phys. Lett. **99**, 1607 (2011).
[3] Y. S. Jia, D. Zhao, M. X. Li, Chin. J. Catal. **39**, 421 (2018).
[4] H. Q. Li, Y. M. Cui, X. C. Wu, Chin. J. Inorg. Chem. **28**, 2597 (2012).
[5] F. Y. Yi, L. He, H. Y. Chen, R. R. Zhao, X. Jiang, Ceram. Inter. **39**, 347 (2013).
[6] Y. Qin, F. Fang, Z. Xie, H. Lin, K. Zhang, X. Yu, K. Chang, ACS Catal. **11**, 11429 (2021).
[7] H. A. Miran, Z. N. Abdullah, M. Altarawneh, M. M. Rahman, A. T. Al-Bayati, E. M-T. Salman, Iran. J. Mater. Sci. Eng. **20**, 1 (2023).
[8] B. Modak, New J. Chem. **46**, 1507 (2022).
[9] Y. Q. Wang, C. Zhang, Y. Liu, M. X. Zhang, F. F. Min, Physica Status Solidi B **256**, 1800574 (2019).
[10] R. H. Zhang, J. Zhao, Y. C. Yang, Z. B. Lu, W. Shi, Comput. Condens. Matt. **6**, 5 (2016).
[11] H. A. Miran, Z. Jaf, I. Khaleel, Phys. Chem. Res. **9**, 553 (2021).
[12] H. A. Miran, Z. Jaf, Papers in Physics **14**, 15 (2022).
[13] M. Miyauchi, M. Takashio, H. Tobimatsu, Langmuir **20**, 232 (2004).

*Corresponding author: yueqin@mail.ustc.edu.cn